

# LOCALIZED SOLUTIONS FOR FLUID INTERFACES VIA METHOD OF VARIATIONAL IMBEDDING

C. I. CHRISTOV \*†

*Laboratoire de Modélisation en Mécanique, CNRS URA 229,  
Université Pierre et Marie Curie (Paris VI), Tour 66,  
4 Place Jussieu, 75252 PARIS CEDEX 05, FRANCE*

## ABSTRACT

The stationary in the moving frame solitary waves of the dissipation modified KdV equation (KdV–KSV) are investigated numerically. The problem of localized solutions is inverse in its nature and it is treated by means of Method of Variational Imbedding (MVI) rendering the original boundary value problem to a higher-order correct in the sense of Hadamard boundary value problem. Several finite-difference approximations of are implemented and discussed. Various kinds of localized solutions are obtained with high accuracy, e.g. three kinds of heteroclinics and two kinds of homoclinics. Heteroclinics exists for continuous spectrum of phase velocity, while each kind of homoclinics appears only for a single eigen value of celerity.

## 1. Posing the Problem

The localized solutions of wave equations are of importance in many different aspects. They are a kind of signature of the system under study. When it is a dissipationless wave equation the localized solitary wave is a result of the balance between nonlinearity and dispersion. In dissipative case it is a sustained by the balance between production and dissipation of energy. A paradigmatic model containing both mentioned balances is the dissipation–modified KdV equation called KdV–KSV. It has appeared in different chapters of the book and we shall not derive it here anew. It is a fourth-order in spatial coordinate Nonlinear Evolution Equation (NEE):

$$u_t + 2\alpha_1 uu_x + \alpha_2 u_{xx} + \alpha_3 u_{xxx} + \alpha_4 u_{xxxx} + \alpha_5 (uu_x)_x = 0 . \quad (1)$$

For the energy

$$E_h \stackrel{def}{=} \int_{-\infty}^{+\infty} \frac{1}{2} u^2 dx ,$$

---

\*Present address: Instituto Pluridisciplinar, Universidad Complutense, Paseo Juan XXIII, No 1, 28040, Madrid, SPAIN

†On leave from the National Institute of Meteorology & Hydrology, Bulgarian Academy of Sciences, Sofia 1184, BULGARIA

the following balance law holds

$$\frac{d}{dt}E_h = \int_{-\infty}^{+\infty} (\alpha_2 + \alpha_5 u) u_x^2 dx - \int_{-\infty}^{+\infty} \alpha_4 u_{xx}^2 d\xi . \quad (2)$$

The first term on r.h.s. is responsible for the energy production (with proper values of Marangoni parameter  $\alpha_5$ ), while the second is the dissipation of energy by the fourth-order diffusion.

### 1.1. Moving-Frame Solution

We seek solutions of type of propagating wave, stationary in the moving frame  $\xi = x - ct$ ,  $\eta(\xi) \equiv u(x - ct)$ . Then eq.(1) is reduced to the following ODE

$$-c\eta' + \alpha_2\eta'' + 2\alpha_1\eta\eta' + \alpha_5(\eta\eta')' + \alpha_3\eta''' + \alpha_4\eta'''' = 0 , \quad (3)$$

where the primes denote differentiation with respect to  $\xi$ . After integration with respect to  $\xi$  the order of eq.(3) is decreased as follows

$$-c\eta + \alpha_2\eta' + \alpha_1\eta^2 + \alpha_5\eta\eta' + \alpha_3\eta'' + \alpha_4\eta''' = C_0 = \text{const} , \quad (4)$$

Since we have not yet specified the numerical values of the coefficients, one can manipulate out the integration constant  $C_0$  merely by means of introducing a new sought function, say  $\zeta = \eta - \eta_0$ , where  $\zeta(\infty) = 0$  and  $\eta_0$  is the solution of the quadratic equation  $-c\eta_0 + \alpha_1\eta_0^2 = C_0$ . For the new function  $\zeta$  one has a homogeneous version of eq.(4), with the only difference that the phase velocity (celerity) is now given by  $(-c + 2\alpha_1\eta_0)$ . In what follows we shall concern ourselves only with the homogeneous equation  $C_0 = 0$  and with solutions that decay to zero at infinity, namely

$$\eta(\infty) = 0 , \quad \eta(-\infty) = \eta_{-\infty} . \quad (5)$$

When  $\eta_{-\infty} = 0$  one has a homoclinic solution (homoclinics, for brevity) and when  $\eta_{-\infty} \neq 0$  one has a heteroclinic solution (heteroclinics, for brevity). It is worth mentioning that the only values of  $\eta_l$  compatible with the equation are  $\eta_l = -c/\alpha_1$  and  $\eta_{-\infty} = 0$ .

Since we are concerned here with the non-trivial generalization of  $KdV$ , we consider the case  $\alpha_4 \neq 0$ . Then without loosing the generality one can set  $\alpha_4 = 1$ , rescaling the coefficients. We did not do that for the sake of convenience when varying the parameters of the problem. For instance, the ratio of coefficient  $\alpha_2$  to  $\alpha_4$  defines in the relative importance of the energy input with respect to the dissipation. At the same time  $\alpha_3/\alpha_4$  specifies the role of dispersion. Sometimes it is easier to vary  $\alpha_4$  instead of varying two or three other parameters.

Note that due to their asymptotic nature, the boundary conditions (5) are equivalent also to infinite number of b.c. on each derivative of  $\eta$ .

In the moving frame the energy balance adopts the form

$$\int_{-\infty}^{+\infty} (\alpha_2 + \alpha_5 \eta) \eta_\xi^2 d\xi - \int_{-\infty}^{+\infty} \alpha_4 \eta_{xx}^2 d\xi = 0 . \quad (6)$$

When obtaining the last equality was acknowledged the fact that  $\eta_{-\infty} = -c/\alpha_1$ .

### 1.2. Normal Form

It is convenient to have eq.(4) in an equivalent form as a system of ODE in normal form, namely

$$\begin{aligned} x' &= y , \\ y' &= z , \\ \alpha_4 z' &= -\alpha_2 y - \alpha_5 x y - \alpha_1 x^2 + c x - \alpha_3 z , \end{aligned} \quad (7)$$

In this formulation the inverse nature of the problem with asymptotic b.c. becomes even more transparent. Now one has to solve a third-order system (7) with six boundary conditions

$$x, y, z \rightarrow 0 \quad \text{for} \quad \xi \rightarrow \infty , \quad x, y, z \rightarrow 0 \quad \text{for} \quad \xi \rightarrow -\infty , \quad (8)$$

It is clear then that it may happen that the boundary value problem (4), (5) (or equivalently: (7), (8)) is overposed and may not have solution for arbitrary values of its coefficients. Since the only free parameter to vary is the unknown celerity  $c$ , then one must consider (4), (5) (or (7), (8)) as a nonlinear eigen-value problem for the eigen parameter  $c$ . This is the main mathematical feature of the problem under consideration. In what follows we concern ourselves with devising a robust method for solution of the said nonlinear eigen value problem.

## 2. Method of Variational Imbedding (MVI)

A new way of constructing robust difference schemes for inverse and incorrect problems was proposed in<sup>4,5</sup> and first applied for finding the homoclinic solution of Lorenz system<sup>4</sup>. To the case of homoclinic solutions of Kuramoto-Sivashinsky (KS) equation, the method was applied in<sup>8,9</sup>. Here we broaden the scope of application of MVI also to heteroclinics.

### 2.1. Sketch of Implementation

The idea of MVI is in replacing the original inverse problem by the problem of minimization of the quadratic functional of the problem. For KdV-KSV this is the functional

$$\int_{-\infty}^{\infty} \Phi^2 d\xi = \min , \quad \Phi \equiv \alpha_4 u''' + \alpha_3 u'' + (\alpha_2 + \alpha_5 u) u' + (\alpha_1 u - c) u \quad (9)$$

The Euler-Lagrange equation for minimization of the above functional reads

$$-\alpha_4 \Phi''' + \alpha_3 \Phi'' - (\alpha_2 + \alpha_5 u) \Phi' + (2\alpha_1 u - c) \Phi = 0 \quad (10)$$

After introduction of (9) into (10) one obtains

$$\begin{aligned} \alpha_4^2 u^{(6)} &+ \left[ -\alpha_3^2 + 2\alpha_2 \alpha_4 + 2\alpha_4 u \right] u'''' + 4\alpha_4 \alpha_5 u' u''' \\ &+ \left[ \alpha_5^2 u^2 + \alpha_2^2 + 2\alpha_3 c + 3\alpha_4 \alpha_5 + 6\alpha_1 \alpha_4 u' + 2\alpha_2 \alpha_5 u - 4\alpha_1 \alpha_3 u - 3\alpha_3 \alpha_5 u' \right] u'' \\ &- \left[ -\alpha_5^2 u^2 - 3\alpha_1 c u + 2\alpha_1^2 u^2 + c^2 \right] u + [\alpha_2 \alpha_5 - 2\alpha_1 \alpha_3] u^2 = 0. \end{aligned} \quad (11)$$

Now one can see that the eq.(11) can support all six boundary conditions on both ends of the interval under consideration. Then it can be effectively quasi-linearized and solved by means of iterative procedure.

The shortcoming of the direct implementation of the MVI is that after the eq. (11) is discretized, one arrives to an algebraic system whose determinant is very small (in fact of order of  $O(h^6)$ , where  $h$  is the spacing). Then any kind of direct elimination procedures will require very long computer words even for not-so-small  $h$ . Our experience in the numerical implementation showed that even calculations with double precision (15 significant digits) failed for (11) when  $h \leq 0.005$ .

## 2.2. Implementation for the Normal Form

A way out of the situation described in the preceding subsection is to use the normal form. Then the Imbedding functional reads

$$\mathcal{I} = \int_{-\infty}^{\infty} \left[ (x' - y)^2 + (y' - z)^2 + \alpha_4 (z' + \alpha_3 z + \alpha_2 y + \alpha_5 xy + \alpha_1 x^2 - cx)^2 \right] d\xi. \quad (12)$$

and Euler-Lagrange equations for this functional are the following

$$\begin{aligned} x'' - \left[ (\alpha_5 y - c)^2 + 2\alpha_1^2 x^2 \right] x &= (z' + \alpha_3 z + \alpha_2 y)(\alpha_5 y - c + 2\alpha_1 x) \\ &+ 3\alpha_1 (\alpha_5 y - c) x^2 + y', \end{aligned} \quad (13)$$

$$y'' - \left[ 1 + (\alpha_2 + \alpha_5 x)^2 \right] y = (z' + \alpha_3 z + \alpha_1 x^2 - cx)(\alpha_2 + \alpha_5 x) + z' - x', \quad (14)$$

$$\begin{aligned} \alpha_4^2 z'' - (1 + \alpha_3^2) z &= -(\alpha_2 + 1 + \alpha_5 x) y' - (\alpha_5 y + 2\alpha_1 x - c) x' \\ &+ \alpha_3 (\alpha_2 y + \alpha_5 xy + \alpha_1 x^2 - cx). \end{aligned} \quad (15)$$

The determinant of the difference approximation to (15) will be now of order of  $O(h^2)$  which allowed us to go to very high resolutions  $h \simeq 10^{-6}$ . The price to be paid is that the number of algebraic equations becomes three times larger than for the direct implementation of the MVI discussed in the preceding subsection. This only poses quantitative limitations on the used computer memory and turns out not to be real obstacle on the way of using grids with large number of points.

### 2.3. The Gist of Variational Imbedding

The essential thing in applying Variational Imbedding is that the Imbedding problem may have more solutions than the original one corresponding to non-zero local minima of variational functional. Then one is to select the solution of the original problem through minimizing the function of one variable  $F(c) = \min_{x,y,z} \mathcal{I}$  to which the functional  $\mathcal{I}$  is reduced after in (12) is introduced the solution of (15). If  $\min_c F(c) = 0$ , then the original problem does possess a solution. If not, this means that the problem under consideration does not possess solution of the sought type (localized waves). The good thing about the MVI is that at each stage of the minimization procedure for  $F$  the solution for  $x, y, z$  is found easily by means of a robust procedure for boundary value problems.

### 3. Difference Scheme

We consider a uniform mesh in the interval  $-\kappa L \leq x \leq (1 - \kappa)L$ , where  $\kappa$  represents the portion of the whole interval that is on the left from the origin of coordinate system and  $L$  is called "actual infinity". We divide the whole interval into  $N - 1$  intervals. By  $N_S = [\kappa N]$  is denoted the grid point where the origin of coordinate system is situated.

We resort to the standard three-point central differences for the first and second derivatives. The very shape of (15) hints at the way the linearization must be effected. The simplest linearization that lives the main diagonal dominating turned out to be the best in numerical sense. The scheme has the following form:

$$\begin{aligned} \frac{1}{h^2}(x_{i+1}^{n+1} - 2x_i^{n+1} + x_{i-1}^{n+1}) &- [(\alpha_5 y^n - c)^2 + 2\alpha_1^2 x^n] x^{n+1} \\ &= 3\alpha_1(\alpha_5 y - c)x^2 + \frac{1}{h}(y_{i+1}^n - y_{i-1}^n) \\ &+ \left[\frac{1}{h}(z_{i+1}^n - z_{i-1}^n) + \alpha_3 z^n + \alpha_2 y^n\right](\alpha_5 y^n - c + 2\alpha_1 x^n), \end{aligned} \quad (16)$$

$$\begin{aligned} \frac{1}{h^2}(y_{i+1}^{n+1} - 2y_i^{n+1} + y_{i-1}^{n+1}) &- -[1 + (\alpha_2 + \alpha_5 x^n)^2] y^{n+1} \\ &= \frac{1}{h}(z_{i+1}^n - z_{i-1}^n) - \frac{1}{h}(x_{i+1}^n - x_{i-1}^n) \\ &+ \left(\frac{1}{h}(z_{i+1}^n - z_{i-1}^n) + \alpha_3 z + \alpha_1 x^2 - cx\right)(\alpha_2 + \alpha_5 x), \end{aligned} \quad (17)$$

$$\begin{aligned} \frac{\alpha_4^2}{h^2}(z_{i+1}^{n+1} - 2z_i^{n+1} + z_{i-1}^{n+1}) &- -(1 + \alpha_3^2)z = -(\alpha_2 + 1 + \alpha_5 x^n)y' \\ &- (\alpha_5 y^n + 2\alpha_1 x^n - c)\frac{1}{h}(x_{i+1}^n - x_{i-1}^n) \\ &+ \alpha_3(\alpha_2 y + \alpha_5 xy + \alpha_1 x^2 - cx). \end{aligned} \quad (18)$$

This difference scheme is coupled by the boundary conditions eq.(19)

$$x_1 = y_1 = z_1 = 0, \quad x_N = y_N = z_N. \quad (19)$$

By renumbering the variables

$$W_{3i-2} \equiv x_i^{n+1}, \quad W_{3i-1} \equiv y_i^{n+1}, \quad W_{3i} \equiv z_i^{n+1},$$

we transform the problem to a linear algebraic problem with seven-diagonal matrix for the unknown difference function  $W$ . For this kind of problems we have devised a special very efficient solver<sup>6</sup> employing Gaussian elimination with pivoting.

The iterations are conducted until convergence in accordance with the criterion:

$$\max_i \{|x_i^{n+1} - x_i^n|, |y_i^{n+1} - y_i^n|, |z_i^{n+1} - z_i^n|\} \leq 10^{-8}. \quad (20)$$

### 3.1. Numerical tests and verifications

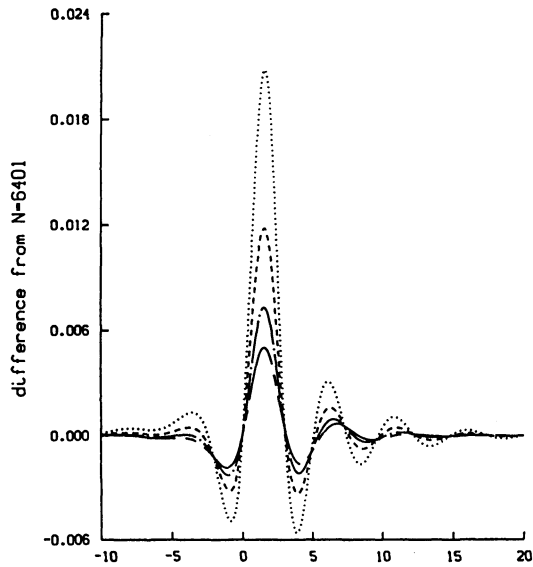
The general consequence of the numerical procedure is as follows

- (1) Starting with smaller  $L$  and increasing it until "something" is found.
- (2) Refining the mesh (increasing the number of points  $N$ ) until the result ceases to change appreciably.
- (3) Adjusting the size of interval  $L$ .
- (4) Briefly repeating the previous steps in order to check whether the newly selected  $L$  leads to improvement of solution.

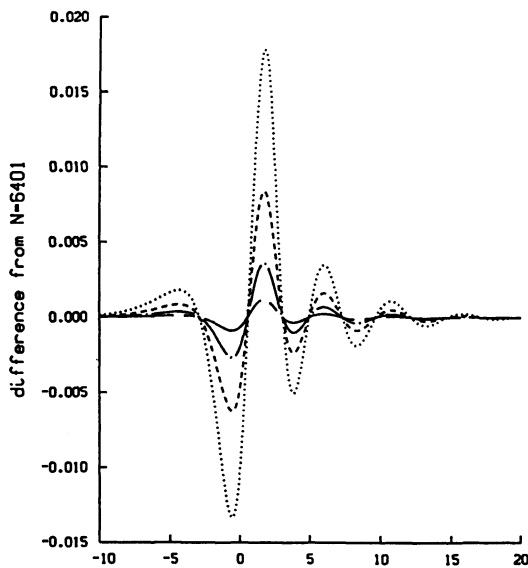
The main mandatory tests with different mesh parameters were duly performed. Here we present some evidence of the good performance of scheme and algorithm.

The influence of resolution is presented in Fig. 1. The comparison between the solutions on different meshes is presented for the original scheme of first-order of approximation with respect to the spatial coordinate. It is clearly seen the convergence toward the reference solution. The comparison for the same resolutions after the Richardson extrapolation is effected show agreement between  $N = 401$  and  $N = 3201$  as good as 0.01% and can not be reasonable presented graphically. In these experiments the "actual infinity"  $L$  is held fixed at 32.

Fig. 2 shows the convergence of solution with the "actual infinity"  $L$ . Note that  $L$  can not be increased very much because in the homoclinic case two humps can appear if  $L$  is large enough to allow the first of them to decay fairly well and to leave the system capable of conceiving another hump. Unlike the two-hump homoclinics discussed later on or the bound states of Ref.<sup>11</sup>, the appearance of two very well separated homoclinic humps is purely numerical effect here when the separation distance is large enough.



(a) heteroclinic solution;



(b) homoclinic solution;

Figure 1: Difference between the solution for different  $N$  from the reference solution with  $N = 6401$ :  $N = 401$  :  $\cdots \cdots$ ;  $N = 801$ :  $-\ - -$ ;  $N = 1601$ :  $-\cdot -$ ;  $c = \infty$ :  $-\ - - -$ . ( $L = 32$ ).

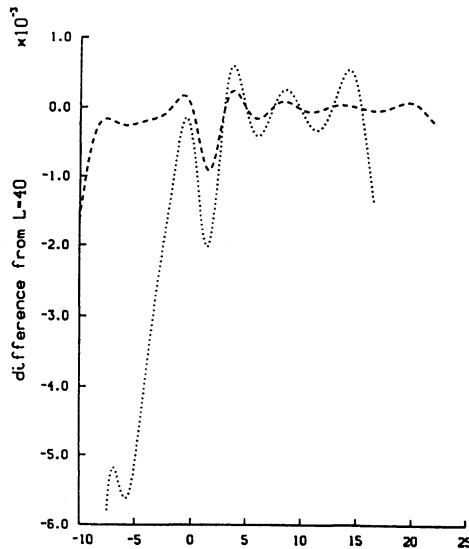


Figure 2: Difference between the solution for different  $L$  from the reference solution with  $L = 40$ :  $L = 24$ :  $\dots\dots\dots$ ;  $N = 32$ :  $-\dots-$ . ( $N = 1601$ ).

The results of these tests are convincing enough that the scheme proposed has good approximation and converges to the solution of the differential problem.

### 3.2. Minimization Algorithm

So, let us consider now the function  $F(c) = \min I_h$ , where the minimum is with respect to the functional arguments  $x(\xi)$ , etc. Respectively,  $c$  stands for the vector of parameters for which an eigen-solution is sought. In the problem under consideration this is a scalar parameter: the celerity of the solitary wave. In order to find the minimum of function  $F(c)$ , the method of golden section is used. We refer the reader to our previous publications<sup>4,9</sup>, for details. Here we merely list the main steps of the algorithm:

- (i) Roughly estimate the interval for  $c$  in which the minimum of  $F(c)$  is located.
- (ii) The golden-section procedure is executed in order to localize the minimum with high precision.
- (iii) If the value of  $F_{min}$  is not equal to zero, or it is not satisfactory close to zero in numerical sense, then some of the parameters of the iterational process (e.g.,  $N$ ,  $L$ , etc.) are changed and steps (i) and (ii) are executed again.

**Conjecture:** A value of order of  $10^{-8}$  is a good approximation to zero for calculations with double precision.

#### 4. Alternative approach: Direct Discretization of the Imbedding Functional

Another way of posing the MVI problem is to discretize the ODE system that enters the Imbedding functional. It has the main advantage that when the solution of the difference imbedding problem is obtained the Imbedding functional must be equal exactly to zero if the solution of the original problem is also obtained. In order to illustrate the idea we consider the following first-order approximation of the ODE, namely

$$I_h = \sum_{i=2}^{N-1} \left\{ \left( \frac{x_{i+1} - x_i}{h} - y_i \right)^2 + \left( \frac{y_{i+1} - y_i}{h} - z_i \right)^2 + \left( \frac{z_{i+1} - z_i}{h} + \alpha_2 y_i + \alpha_5 y_i x_i + \alpha_3 z_i - c x_i + \alpha_1 x_i^2 \right)^2 \right\}.$$

Here, for the sake of convenience, the Newton quasilinearization is performed already in the functional.

The Euler-Lagrange equations for the function of many variables (21) express the necessary conditions for a local minimum, namely

$$\frac{\partial I_h}{\partial x_i} = 0, \quad \frac{\partial I_h}{\partial y_i} = 0, \quad \frac{\partial I_h}{\partial z_i} = 0, \quad (21)$$

which in this case give

$$\begin{aligned} \frac{1}{h^2}(z_{i+1} - 2z_i + z_{i-1}) - (1 + \alpha_3^2)z_i + \frac{1}{h}(y_{i+1} - y_i) - \frac{\alpha_3}{h}(z_{i+1} - z_i) \\ + \frac{1}{h}(\alpha_2 + \alpha_5 x_i)(y_i - y_{i-1}) - \alpha_3(\alpha_2 + \alpha_5 x_i)y_i \\ = \alpha_3(\alpha_1 x_i^2 - c x_i) - \frac{1}{h}[(\alpha_1 x_i^2 - c x_i) - (\alpha_1 x_{i-1}^2 - c x_{i-1})] \end{aligned} \quad (22)$$

$$\begin{aligned} \frac{1}{h^2}(y_{i+1} - 2y_i + y_{i-1}) - [1 + (\alpha_2 + \alpha_5 x_i)^2]y_i + \frac{1}{h}(x_{i+1} - x_i) - \frac{1}{h}(z_i - z_{i-1}) \\ - (\alpha_2 + \alpha_5 x_i)\frac{1}{h}(z_{i+1} - z_i) - (\alpha_2 + \alpha_5 x_i)\alpha_3 z_i \\ = (\alpha_2 + \alpha_5 x_i)(\alpha_1 x_i^2 - c x_i) \end{aligned} \quad (23)$$

$$\begin{aligned} \frac{1}{h^2}(x_{i+1} - 2x_i + x_{i-1}) - (\alpha_5 y_i - c + 2\alpha_1 x_i)^2 x_i - \frac{1}{h}(y_i - y_{i-1}) \\ = (\alpha_5 y_i - c + 2\alpha_1 x_i) \left[ \frac{1}{h}(z_{i+1} - z_i) + \alpha_3 z_i + \alpha_2 y_i - \alpha_1 x_i^2 \right] \end{aligned} \quad (24)$$

In order to alleviate the presentation we do not explicitly write the superscripts referring to the iterative stage. We merely note that the linearization is performed according to the same principles as for the difference scheme in the previous Section.

This scheme is  $O(h)$  and second order is achieved by means of Richardson extrapolation. This turns out to be the cheapest way, because the higher-order schemes require more iterations for convergence. Since, the calculations on two different meshes are mandatory, why not to use them to increase the accuracy of the scheme? Once again, the boundary conditions for the difference scheme are (19)

## 5. Results for heteroclinics (kinks/ shocks/ hydraulic jumps/ bores)

It can be expected that due to the difference between levels of fluid surface before and after the hydraulic jump, the energy balance (6) may be satisfied for arbitrary magnitude of the jump (and hence for each celerity  $c$ ). Indeed, our calculations show that this is case. We have obtained heteroclinic solutions for each value of  $c > 0.3$  and most of the cases more than one solution for a given celerity. Roughly the heteroclinic solutions fall into three main groups ("genders"). There is no proof that these are the only classes of kink solutions. Although weakly nonlinear, the problem under consideration is *nonlinear* and possesses extremely rich phenomenology<sup>12,13</sup>.

### 5.1. Kinks of first gender. Self-similarity with respect to celerity

The kinks of first gender have only one front (Fig. 3). Numerically we have found them for  $1 \leq c \leq 64$ , and there are reasons to believe that the interval of celerity extends up to infinity. The following derivations confirm this supposition. For nontrivial values of celerity one can introduce the transformation

$$\eta = cv \left( \frac{x}{c^{1/3}} \right), \quad \eta' = c^{4/3} v' \left( \frac{x}{c^{1/3}} \right), \quad (25)$$

Then eq.(1) can be recast as follows

$$-v + \alpha_1 v^2 + c^{-2/3} \alpha_2 v' + \alpha_3 c^{-1/3} v'' + \alpha_4 v''' = 0. \quad (26)$$

Now it is clear that for  $c \gg 1$  the terms containing  $v', v''$  are negligible, i.e., the scaled solution for  $c \gg 1$  should not depend on  $c$ ! Fig. 3 confirms that with the increase of  $c$  the solution tends to the solution of (26). Be noted that the curve in Fig. 3 marked as  $c = \infty$  is the solution to eq.(26) with  $c^{-1/3} \equiv 0$ . It goes without saying that the solution of eq.(26) is obtained in its turn by the method of variational imbedding.

### 5.2. Effect of dispersion on heteroclinic solution of first gender

Our calculations with nontrivial dispersion parameter  $\alpha_3 \neq 0$ , showed that increasing the dispersion parameter makes the shape of the bore more undular. This is

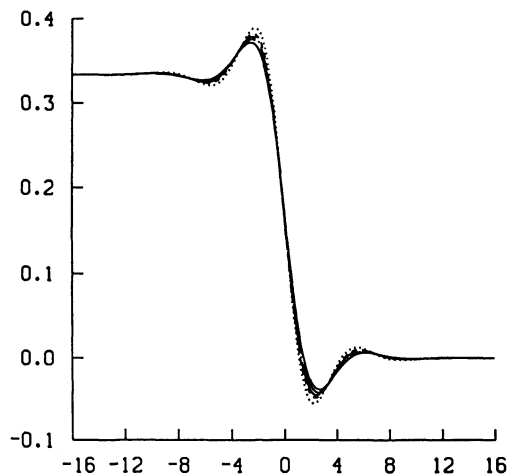
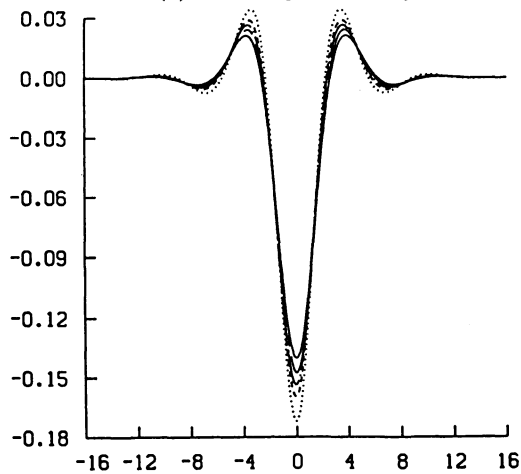
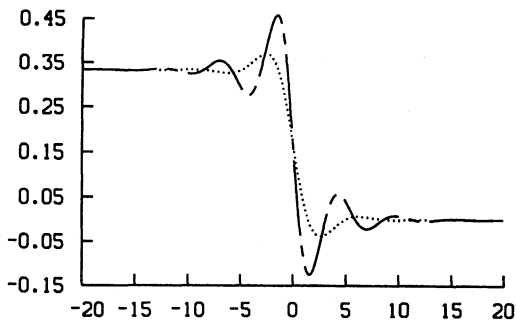
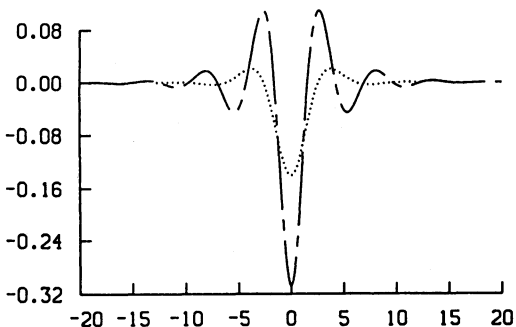
(a) kink shape scaled by  $c$ ;(b) shape of derivative scaled by  $c^{4/3}$ .

Figure 3: The self-similarity of solution (abscissa is scaled by  $c^{1/3}$ ) for  $\alpha_1 = 3, \alpha_2 = 1, \alpha_3 = 0, \alpha_4 = 1$  with increasing the celerity :  $c = 8$  :  $\cdots\cdots\cdots$ ;  $c = 16$  :  $-\cdots-$ ;  $c = 27$  :  $-\cdot-\cdot-\cdot$ ;  $c = 64$  :  $-\cdot-\cdot-$ ;  $c = \infty$  :  $\text{—}$ .



(a) kink shape



(b) shape of first spatial derivative

Figure 4: Role of dispersions for kinks for  $c = 1$ :  $\cdots - \alpha_3 = 0$ ;  $--- - \alpha_3 = 1$ . Resolution  $N = 1601$ .

well seen in Fig. 4. Here we have a conspicuous difference from the homoclinic case for which the cited works<sup>2,3,10,14</sup> and our calculations as well (see below) unequivocally state that the dispersion reduces the undulations of the solution.

### 5.3. Kinks of second gender

Here belong the hydraulic jumps with double front. In the range of celerity they occupy roughly the region  $0.5 \leq c \leq 8$  and peacefully coexist with the kinks of first gender. Their shape is presented in Fig. 5. Note that contrary to the previous case and contrary to the intuitive expectations, the relative importance of the undulations *decreases* with the increase of the celerity  $c$ ! It is another story that perhaps, the second gender becomes unstable as initial value problem and is never realized in nature or in direct numerical simulations, involving time.

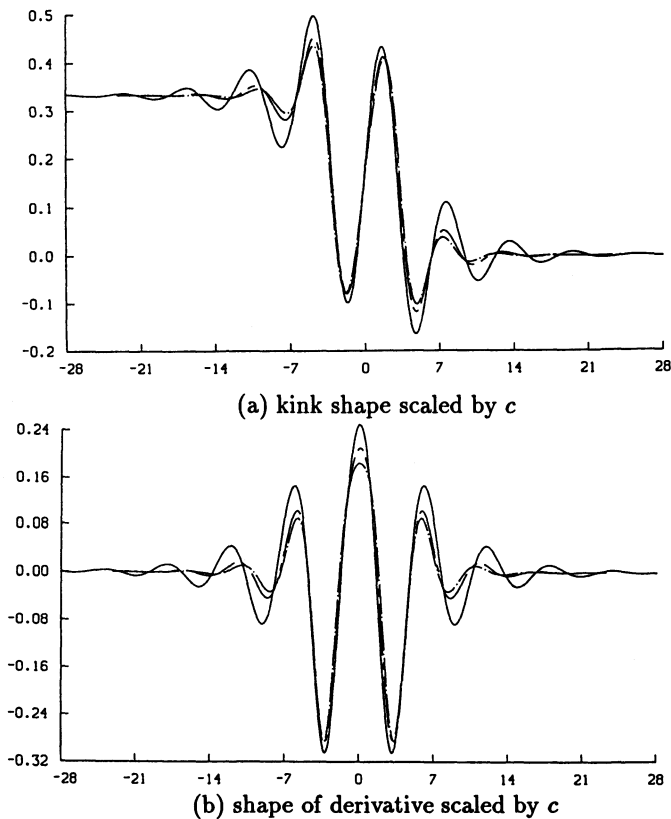


Figure 5: Kinks of second gender (abscissa is not scaled): — · — · —  $c = 1.4$ ; — — —  $c = 1$ ; — — —  $c = 0.5$ . Resolution  $N = 1601$ , interval  $L = 32$ .

#### 5.4. Kinks of third gender

We consider as belonging to the third gender, the kinks with triple main slope or which is the same – with derivative that has a negative minimum in the center of kink. Note that the previous case had positive derivative in the center. The shape of derivative for this sub-class is shown in Fig. 6. It is seen that the shape becomes significantly smoother for the large value of celerity  $c = 8$ .

For very small values of celerity  $c < 0.5$  the kinks of third gender lose their symmetry (see Fig. 7). We had obtained some results even for  $c = 0.3$  and they were once again non-symmetries for the derivative, just like the case  $c = 0.4$  which is presented in Fig. 7. In fact they look very much like linear waves, although they are localized structures. Because of decreased role of the nonlinearity at low celerities,

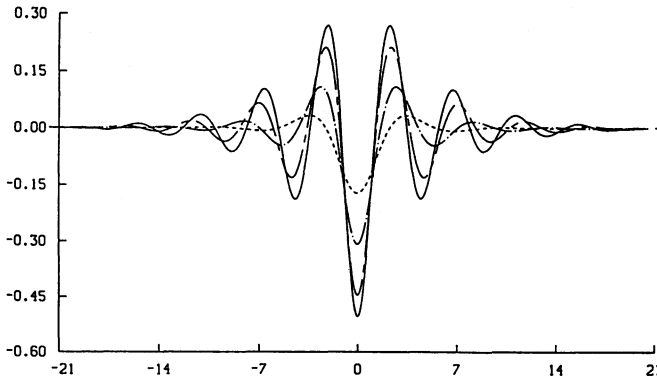


Figure 6: Kinks of third gender (abscissa is not scaled). Shape of derivative scaled by  $c$ : - - - -  $c = 8$ .; · - - · -  $c = 1$ .; - - - -  $c = 0.5$ ; ————  $c = 0.4$ . Resolution  $N = 3201$ , Interval  $L = 56$ .

the localization is not so pronounced and the “actual infinity” has to be of order of  $L = 200$  in order to harbor the winged localized creature. The latter reduces the number of points per wavelength and we deem those results not accurate enough.

## 6. Results for hump solutions (homoclinics)

The problem of identification of a homoclinics is much more complicated and needs special treatment. In fact it is an intrinsically nonlinear eigen-value problem. Here MVI is at its most. The main advantage is that a solution to the Euler-Lagrange system can always be found, regardless of the fact whether a solution to the original problem exists. Then one can smoothly proceed with changing the eigen-value parameter until the value of the minimum  $\mathcal{I}$  or  $I_h$  approaches “numerical” zero. If this happens, then the original problem does possess a nontrivial eigen-solution. If not, then this is a proof, that a solution of the sought type does not exist.

### 6.1. Evasive one-hump homoclinics of KS

It turned out that a hump shape propagating to the right exists in KSE only for a single value of phase velocity  $c = 1.216$ <sup>9,15</sup> although in some papers<sup>1,8,14</sup>, the possibility that the spectrum could be continuous was not excluded. We provide here in Fig. 8 an explanation of this purely numerical effect. As it has turned out (see the previous Section), a heteroclinics does exist for continuous spectrum of phase velocities. In the same time it has exactly the same undulate forerunner as the homoclinics-to-be. Then if one matches a function exponentially decaying towards  $-\infty$  (a “tail”) to an arbitrary heteroclinics, one obtains a homoclinic shape which satisfies the equation everywhere, save the point of matching the tail where only the

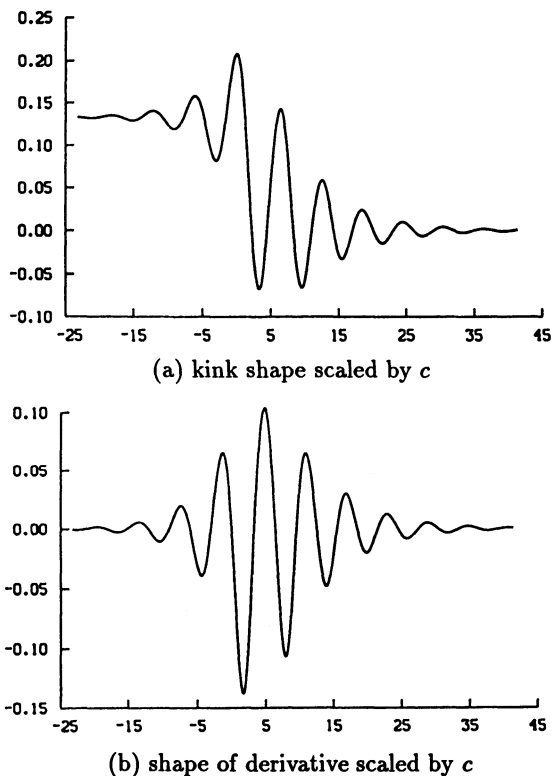


Figure 7: Degenerating kinks of third gender for  $c = 0.4$ . Resolution  $N = 1601$ , interval  $L = 96$ .

second derivative is discontinuous. The function and first derivative are continuous due to the matching and the third derivative is then automatically continuous due to the fact that the equation does not contain second derivative. Then it is clear, that such a shape would give a very small residual if introduced into the equation (for the case  $c = 1$  in Fig. 8 the integral of the square of the residual is about  $4 \cdot 10^{-3}$ ). There is no surprise then, that if calculations are conducted with single precision, the artificial homoclinics could be mistaken for a real solution to the KS. It took us special effort<sup>9</sup> using refined calculations with double precision to rule out the homoclinics, except for the value  $c = 1.216$  when the residual goes down to  $10^{-9}$ . Note that the residual for the heteroclinic solution in Fig. 8 has always been of order  $10^{-12}$  (see previous section).

Here is to be mentioned, that when the approximation of the differential equations of MVI are used, the value of functional is of order of *truncation error* and can never

Table 1: Celerity as function of dispersion parameter

$\alpha_3$	$c$	$10^7 \cdot \text{Funct.}$
0.5	1.6809	1.098274
1.0	2.1802	1.767140
2.0	3.2872	6.666997
3.0	4.4348	5.359481
4.0	5.5944	5.630318

be closer to zero than, say  $10^{-5}$  for practical size of the mesh.

### 6.2. Influence of dispersion on one-hump homoclinics

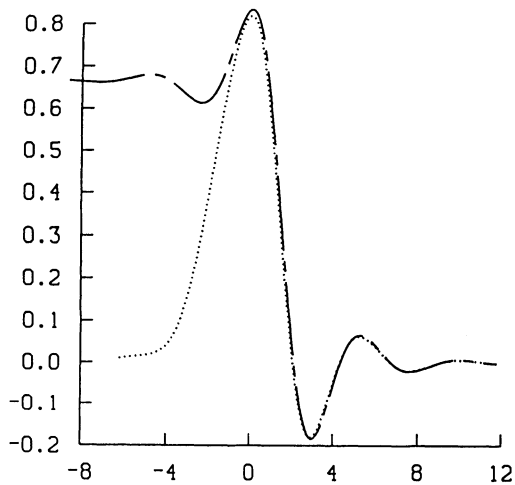
As mentioned by many authors<sup>2,3,14,10</sup>, the dispersion may play stabilizing role in KdV-KSV equation. Indeed we solved the eigen-value problem for different values of  $\alpha_3$ . Naturally, the obtained eigen-values for celerity are different. For larger values of the dispersion parameter, the shape of the homoclinic solution approaches the well-known *sech*-solution (see, e.g., <sup>7,10,14</sup>). The only difference is that the dissipation provides for celerity selection and hence the one-hump shape exists only for a single value of celerity. Representative sample of eigen-values is given in Table 1. The respective shapes of the solution are presented in Fig. 9 after scaled by the celerity  $c^\dagger$ . One sees that even for  $\alpha_3 = 0.5$  the wave forerunner is much reduced with comparison with the homoclinics for  $\alpha_3 = 0$  (see Fig. 8). For  $\alpha_3 = 4$  the shape virtually coincides with the *sech*-shape corresponding to that value of celerity.

To conclude our investigation of the influence of the dispersion on the one-hump solution we can mention that in case of homoclinic shapes it plays laminarizing role, while for the kinks it makes the heteroclinics wavier.

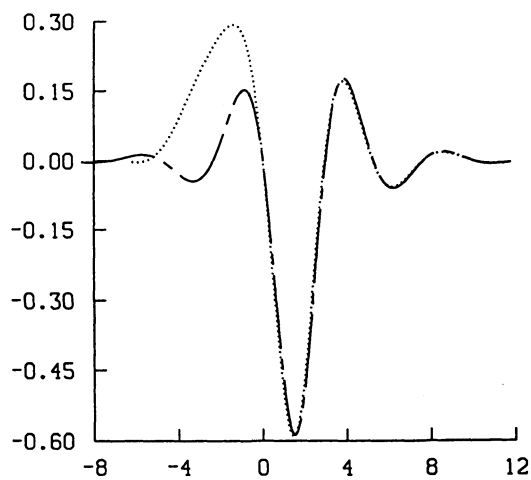
### 6.3. Two-hump homoclinics

Apart from stabilizing the homoclinic orbits, the influence of dispersion is felt also in the fact that it makes the two-hump homoclinics more stable when MVI is applied, in the sense that the minimum achieved is much deeper. We discovered that another solution appears for  $\alpha_3 \neq 0$  which has two humps. This is hardly interpreted as a bound state of two one-hump solutions as these encountered in our direct numerical simulations of KdV-KSV<sup>11</sup>. Rather this is a more intricate homoclinic shape (see Fig. 10) for which the forerunning hump is of conspicuously larger amplitude than the lagging one, the latter being quite similar to the one-hump solution from Fig. 9. Yet the larger amplitude of the two-hump solution does not preclude higher celerity.

<sup>†</sup>A similar picture has been presented in our work<sup>16</sup> which apparently differs from the figure here. The difference is that in Ref.<sup>16</sup> the abscissa is also scaled by  $c^{1/3}$ , similarly to the above discussed case of kinks (jumps).



(a) kink shape



(b) the shape of derivative.

Figure 8: Comparison of the real heteroclinics and the pseudo-homoclinics of KS for  $c = 2$ ,  $n = 1601$ ,  $L_{kink} = 48$ ,  $L_{bump} = 28$ .

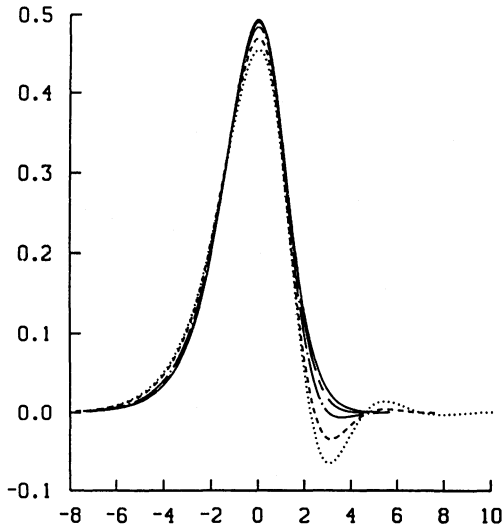


Figure 9: Influence of dispersion on shape of the one-hump homoclinic solution of KdV-KSV:  $\cdots\cdots\cdots$   $\alpha_3 = 0.5$ ;  $-----$   $\alpha_3 = 1.0$ ;  $-\cdot-\cdot-\cdot-$   $\alpha_3 = 2.0$ ;  $-----$   $\alpha_3 = 3.0$ ;  $—————$   $\alpha_3 = 4.0$ . Resolution  $N = 1601$ ,  $N_S = 701$ .

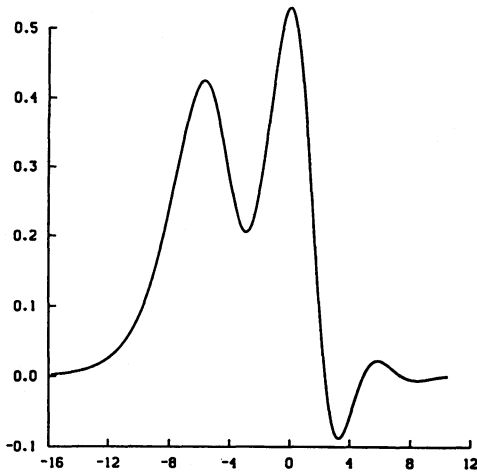


Figure 10: Two-hump homoclinic solution for  $\alpha_3 = 0.5$ . Eigen-value for celerity  $c = 1.075$ , length of interval  $L = 48$ , resolution  $N = 16001$ ,  $N_S = 801$ .

On the contrary, the celerity  $c = 1.075$  of the two-hump solution is lower than the celerity  $c = 1.216$  of the one-hump localized wave.

**Acknowledgements** Author benefited from illuminating discussions with M. G. Velarde and G. A. Maugin. A sabbatical fellowship from the Spanish Ministry of Science and Education is gratefully acknowledged. The main part of this work was done when the author was at Laboratoire de Modélisation en Mécanique, CNRS URA 229, Université Paris VI, France.

## 7. References

1. H.-C. Chang, Evolution of Nonlinear Waves on Vertically Falling Films – A normal Form Analysis, *Chem. Engn. Sci.*, **42** (1987) 515–533.
2. H.-C. Chang, E. A. Demekhin, and D. I. Kopelevich, Laminarizing effect of dispersion in an active-dissipative nonlinear medium. *Physica, D* **63** (1993) 299–320.
3. H.-C. Chang, E. A. Demekhin, and D. I. Kopelevich, Nonlinear evolution of waves on a vertically falling film, *J. Fluid Mech.*, **250** (1993) 433–480.
4. C. I. Christov, A Method for Identification of Homoclinic Trajectories, In: *Proc. 14-th Spring Conf. Union of Bulg. Mathematicians*, (Union of Bulgarian Mathematicians, Sofia, 1985) pp. 571–577.
5. C. I. Christov, Method of variational imbedding for elliptic incorrect problems. *Comp. Rend. Acad. Buld. Sci.*, **39(12)** (1986) 23–26.
6. Christov C.I., Gaussian elimination with pivoting for multidagonal systems, *Internal Report, University of Reading*, **4** (1994).
7. C.I. Christov, Numerical Investigation of the Long-time Evolution and Interaction of Localized Waves, *These proceedings*.
8. C. I. Christov and V. P. Nartov, Application of the Method of Variational Imbedding for Calculating Shapes of Solitons on Falling Thin Films, In: *Proc. Conf. on Centenary of Academician L. Tchakalov*, (Samokov, Bulgaria, 1986), pp. 135–142. (in Russian)
9. C. I. Christov and M. G. Velarde, On Localized Solutions of an Equation Governing Benard-Marangoni Convection, *Appl. Mathem. Modelling*, **17** (1993) 311–320.
10. C. Elphick, G. R. Ierley, O. Regev, and E. A. Spiegel, Interacting localized structures with galilean invariance, *Phys. Rev.*, **A44** (1991) 1110–1122.
11. C. I. Christov and M. G. Velarde, Solitons and Dissipation, *These Proceedings*
12. J. M. Hyman and B. Nicolaenko, The Kuramoto-Sivashinsky equation: a bridge between PDE's and dynamical systems, *Physica, D* **18** (1986) 113–126.
13. J. M. Hyman and B. Nicolaenko, Coherence and chaos in Kuramoto-Velarde equation, In: *Directions in Partial Differential Equations*, Eds. M. G. Grandall, P. H. Rabinovitz and R. E. L. Turner, (Academic Press, 1987), pp. 89–111.

14. T. Kawahara and S. Toh, Pulse interactions in an unstable dissipative-dispersion nonlinear system, *Phys. Fluids*, **31** (1988) 2103-2111.
15. O. Yu. Tzvelodub, Stationary Propagating Waves on a Thin Film Falling down a Vertical Wall, In: *Wave Processes in Two-Component Media*, Ed. V. E. Nakoryakov, (Novosibirsk, 1980), pp. 47-63. (in Russian)
16. M. G. Velarde, N. N. Garazo and C. I. Christov, Localized structures and solitary waves excited by interfacial stresses. In: *Spontaneous Formation of Space-Time Structures and Criticality*, Eds. T. Riste and D. Sherrington, (Kluwer, Dordrecht, 1991), pp. 263-272.